Research Square

Preprints are preliminary reports that have not undergone peer review.
They should not be considered conclusive, used to inform clinical practice,
or referenced by the media as validated information.

Seismic Response of Non-displacement Pile Group in Dry Sand: Localized Pile–Soil Deformation Incompatibility Revealed by Geotechnical Centrifuge Tests

pengkun Rao
China Institute of Water Resources and Hydropower Research
xuedong Zhang
ytzxd@iwhr.com
China Institute of Water Resources and Hydropower Research
rui Wang
China Institute of Water Resources and Hydropower Research
yanpeng Sun
China Institute of Water Resources and Hydropower Research
weizhe Meng
China Institute of Water Resources and Hydropower Research

Research Article

Keywords: Non-displacement pile group, Geotechnical centrifuge shaking table test, Kinematic incompatibility, Acceleration response reversal, Shear stress–strain hysteresis loops

Posted Date: November 13th, 2026

DOI: https://doi.org/10.21203/rs.3.rs-11399494/v1

License: This work is licensed under a Creative Commons Attribution 4.0 International License.
Read Full License

Additional Declarations: No competing interests reported.

Seismic Response of Non-displacement Pile Group in Dry Sand: Localized Pile–Soil Deformation Incompatibility Revealed by Geotechnical Centrifuge Tests

Abstract

This study investigates the seismic response of a capped 3 × 6 non-displacement pile group in dry sand, with particular emphasis on localized pile–soil kinematic incompatibility. Centrifuge shaking-table tests were conducted on unreinforced and pile-reinforced ground under input motions of 0.18g, 0.22g, and 0.26g. Within the significant duration defined by 5%–95% of the cumulative Arias intensity, the pile group reduced PGA amplification under the 0.18g and 0.22g motions. Under the 0.26g motion, however, the shallow reinforced soil exhibited greater acceleration amplification than the unreinforced soil, whereas the mitigating effect persisted at depth. Shear stress–strain loops further revealed increased cyclic strain and reduced apparent stiffness in the shallow inter-pile soil. This localized reversal is attributed to pile-cap inertia, repeated lateral pile–soil interaction, and the growing stiffness contrast between the rigid pile–cap system and the softened sand. These findings indicate that large capped pile groups may restrain the overall ground response while intensifying deformation locally. Seismic design and performance assessment should therefore account for the depth-dependent response of the inter-pile soil and the potential for shallow amplification under strong shaking.

Keywords

Non-displacement pile group; Geotechnical centrifuge shaking table test; Kinematic incompatibility; Acceleration response reversal; Shear stress–strain hysteresis loops

1 Introduction

Non-displacement piles are widely employed in ground improvement and foundation engineering because they provide effective reinforcement while limiting disturbance to the surrounding soil. When connected by a pile cap, they form a pile-group foundation with greater load-carrying capacity and overall stability than an isolated pile. Under seismic loading, however, the dynamic response of pile foundations remains a major concern. Post-earthquake observations have consistently shown that pile damage tends to concentrate near the pile head, at interfaces between soil layers with pronounced stiffness contrasts, and within liquefiable or highly deformable strata. In particular, kinematic bending induced by abrupt variations in soil stiffness is widely recognized as an important mechanism of localized pile damage (Nikolaou et al. 2001; Tokimatsu et al. 2005).

Despite extensive research, it remains uncertain whether pile-group reinforcement invariably improves the seismic performance of the surrounding ground. Some studies emphasize the beneficial stiffness contribution of the reinforced zone, in which the piles and surrounding soil interact to reduce ground deformation and pile bending demand (Sawamura et al. 2021; Padmanabhan et al. 2024). In contrast, other studies indicate that pronounced kinematic and inertial interactions may redistribute seismic demand or locally amplify the soil response when the pile–cap system and the surrounding soil deform incompatibly (Tokimatsu et al. 2005; Hussien et al. 2016). The seismic effect of pile reinforcement therefore cannot be interpreted solely as stiffness enhancement, but should instead be regarded as the outcome of coupled soil–pile–cap interaction.

Analytical and numerical studies have clarified key aspects of pile–soil kinematic interaction. Fan et al. (1991) showed that motion transmitted to a capped pile group may differ from free-field motion, while Stacul et al. (2022) demonstrated that soil nonlinearity, stiffness degradation, and pile yielding can modify the kinematic response. However, local predictions remain sensitive to constitutive assumptions and interface treatment. Neglecting pile–soil slip or separation may underestimate kinematic demand (Aghamolaei et al. 2024a, b), whereas loading frequency and nonlinear free-field response can strongly affect pile displacement and internal forces (Ahmadi et al. 2025; Rodríguez-Galván et al. 2026). Even models calibrated against centrifuge data may not fully reproduce coupled kinematic and interface behavior (Lee et al. 2026). Numerical analysis is therefore informative, but localized contact loss, repeated compression, and deformation concentration still require experimental verification.

Shaking-table tests provide more direct evidence of deformation incompatibility. Reported phenomena include gap opening, repeated pile–soil contact, localized acceleration peaks, and differences between near-pile and free-field deformation (Chau et al. 2009; Tamura et al. 2021; Aghamolaei et al. 2024a, b). Zhang et al. (2025) observed a transition from linear to nonlinear interaction with increasing shaking intensity, while Yang et al. (2026) identified phase differences and relative motion between piles

and adjacent soil. He et al. (2026) further described a cyclic compression–detachment mechanism controlled by relative displacement. Nevertheless, 1-g tests cannot reproduce prototype self-weight stresses, and most studies have focused on single piles, slopes, or specialized layered ground rather than soil enclosed within large pile groups.

Centrifuge shaking-table testing is better suited to this problem because it restores prototype stress conditions. Existing studies show that pile–soil relative motion is influenced by excitation frequency (Hussien et al. 2016), displacement phase relation (Tran et al. 2022), ground-induced kinematic force (Yun and Han 2023), and pile–cap connection conditions (Zheng et al. 2024). More broadly, centrifuge studies have focused mainly on single piles or regular 2 × 2 and 3 × 3 groups, with limited attention to the depth-dependent acceleration, shear stress, and shear strain of inter-pile soil within large, non-square pile–cap systems.

To address this gap, comparative centrifuge shaking-table tests were conducted on unreinforced dry sand and dry sand reinforced with a capped 3 × 6 non-displacement pile group. The depth-dependent acceleration, shear stress, and shear strain of the inter-pile soil were examined under different shaking intensities. The study investigates whether the overall restraint observed under mild-to-moderate shaking develops into localized shallow response reversal under strong shaking. Shear stress–strain hysteresis loops were used to relate this transition to cyclic shear deformation, apparent stiffness degradation, and localized pile–soil kinematic incompatibility.

2 Centrifuge Shaking Table Tests

2.1 Test Facilities and Model Container

Centrifuge shaking table tests were performed at the China Institute of Water Resources and Hydropower Research, utilizing the LXJ-4-450 geotechnical centrifuge and the R500B shaking table (Fig.1).

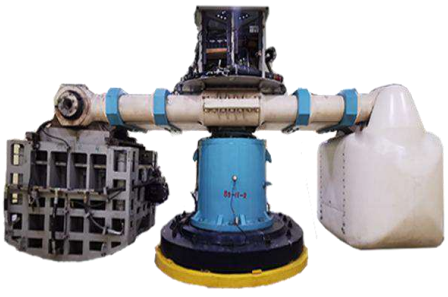


Fig.1. LXJ-4-450 geotechnical centrifuge and R500B centrifuge shaking table.

An equivalent shear beam container measuring 780 mm × 350 mm × 500 mm was used, and acceleration was recorded using PCB-352A24 accelerometers with a ±50g range and a frequency response of 1–8000 Hz. as depicted in Fig.2.



Fig.2. Equivalent shear beam model container and accelerometer

2.2 Experimental Design and Sensor Layout

Table 1.Test Plan

Model ID	Test Case ID	Centrifugal Acceleration	Ground Type	Peak Acceleration (Prototype)
M1	M1-1	40g	Unreinforced dry sand ground	0.18g
	M1-2			0.22g
	M1-3			0.26g
M2	M2-1		Dry sand ground reinforced with a non-displacement pile group	0.18g
	M2-2			0.22g
	M2-3			0.26g

As summarized in Table 1, the unreinforced and pile-reinforced models were each subjected to broadband motions with prototype PGAs of 0.18g, 0.22g, and 0.26g. The 36-s horizontal motion was applied along the longitudinal axis of the container. Identical vertical accelerometer arrays were installed in the free field of M1 and the inter-pile soil of M2.

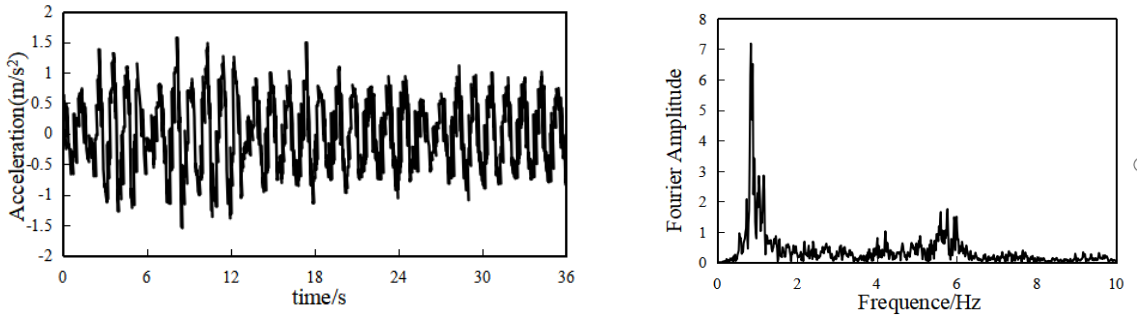
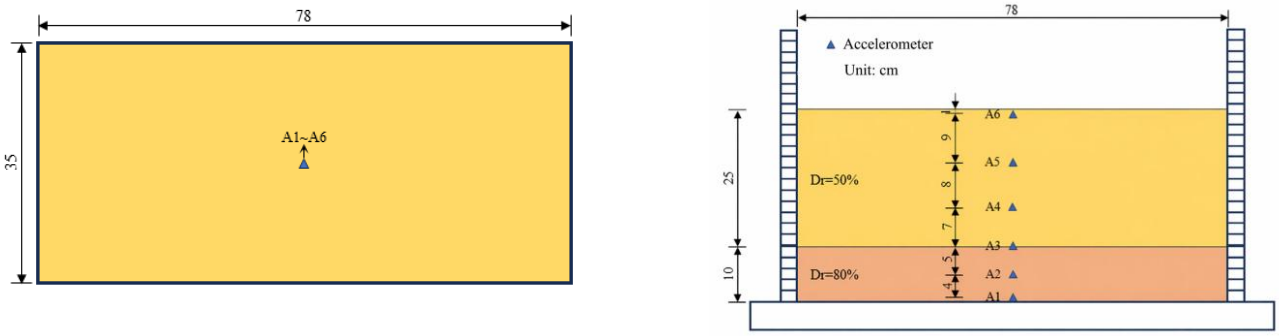
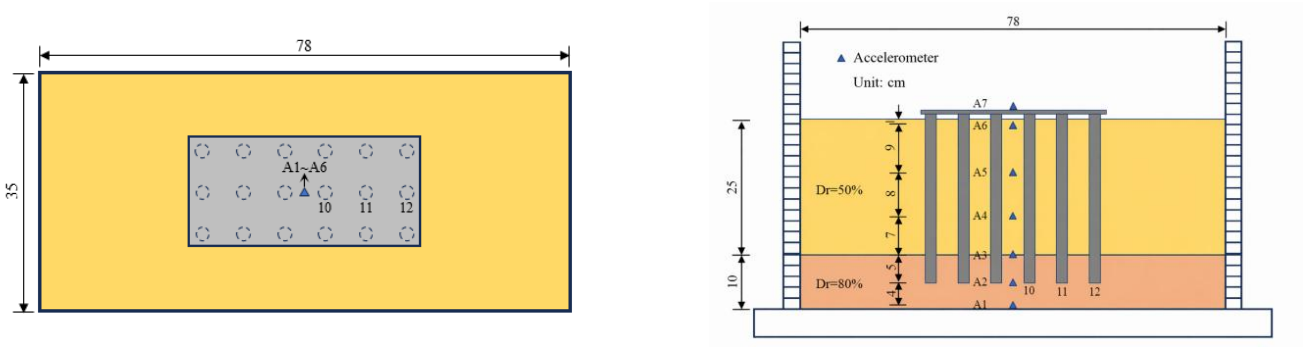


Fig.3. input earthquake record: (a) acceleration time history; (b) Fourier spectrum



(a) (b)

Fig.4. Accelerometer layout in the unreinforced dry sand ground model: (a) plan view; (b) front view



(a) (b)

Fig.5. Accelerometer layout in the dry sand ground reinforced with a non-displacement pile group: (a) plan view; (b) front view

2.3 Materials and Model Preparation

The test piles and pile cap were fabricated from aluminum alloy, with their mechanical properties summarized in Table 2. The pile group comprised 18 cylindrical piles arranged in a 3 × 6 configuration. Each pile had a diameter of 2 cm and a length of 31 cm, spaced at a center-to-center distance of 6 cm. The pile cap measured 34 cm × 16 cm × 0.8 cm. To ensure the integral behavior of the pile group–cap system, each pile was rigidly bolted to the cap, as illustrated in Fig.6.

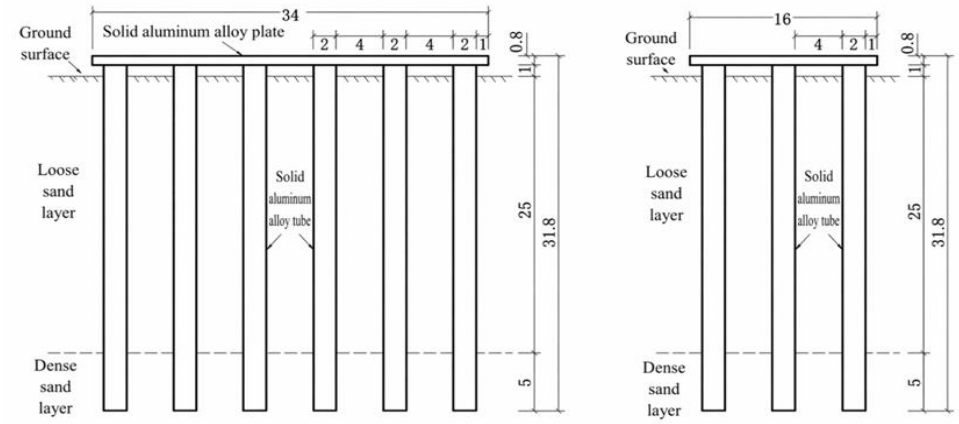


Fig.6.Scaled model of the 3 × 6 non-displacement pile group

Table 2. Mechanical properties of the aluminum alloy

Tensile strength (MPa)	Yield strength (MPa)	Elastic modulus (GPa)	Poisson's ratio	Elongation(%)
220	90	70	0.33	15

Fujian standard sand was used as the foundation soil in this study. The measured basic physical properties of the sand are summarized in Table 3, and its particle size distribution curve is presented in Fig.7

Table 3.Physical properties of Fujian standard sand

Material	Gs	D_{60}/mm	C_u	C_c	$\rho_{d,max}$(g/cm^3)	$\rho_{d,min}$(g/cm^3)
Fujian standard sand	2.664	0.49	1.75	1.29	1.791	1.606

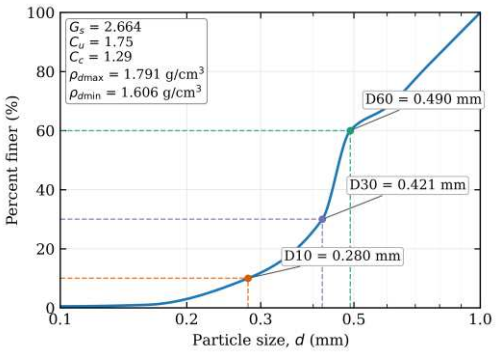
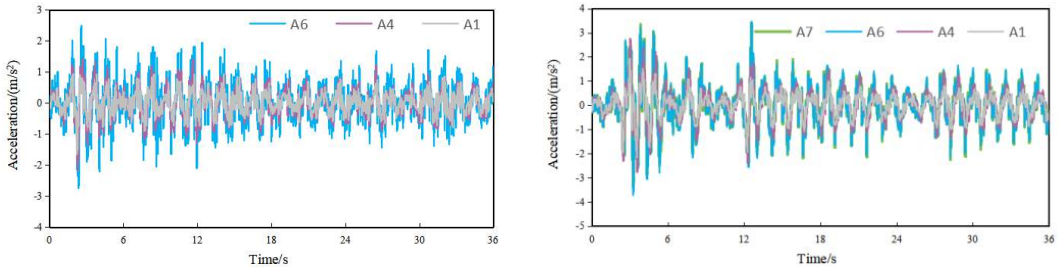


Fig.7.Grain size distribution curve of Fujian standard sand

3 Results and Discussion

3.1 Acceleration Response of Soil Layers

Figure 8 presents the representative acceleration time histories of the two ground models under the 0.26g input motion. To reduce electromagnetic interference generated during centrifuge shaking-table operation, the raw acceleration records were processed in SeismoSignal using a high-pass filter with a cut-off frequency of 0.25 Hz. Figures 8(a) and 8(b) show the acceleration responses of the unreinforced dry sand model M1-3 and the pile-reinforced model M2-3, respectively.



(c)M1-3 (f)M2-3

Fig.8.Acceleration time histories of the unreinforced and pile-reinforced dry sand grounds.

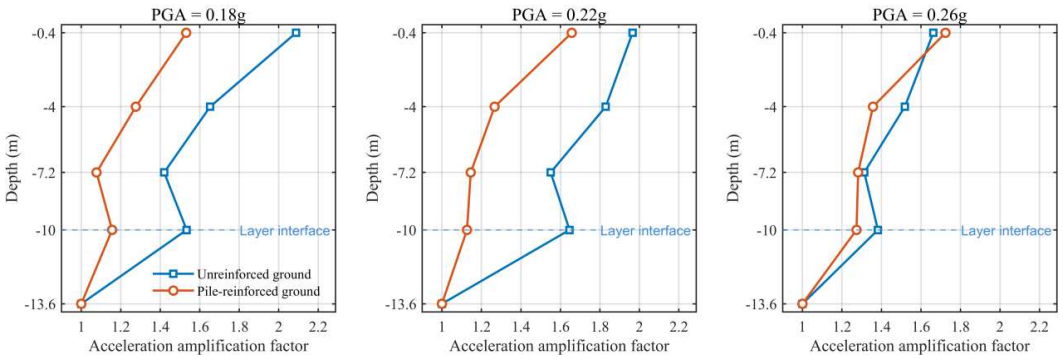


Fig.9.PGA amplification factor profiles of the unreinforced and pile-reinforced grounds

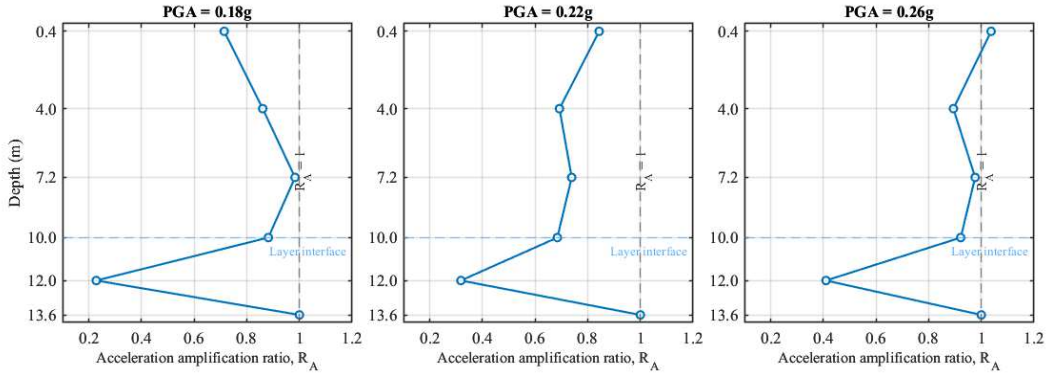


Fig.10.Depth profiles of the PGA amplification ratio between the pile-reinforced and unreinforced grounds within the Arias-intensity-based 5%–95% significant duration.

As illustrated in Fig.9, both ground conditions exhibit upward acceleration amplification toward the surface, with the overall acceleration response intensifying as the input motion increases. As shown in Fig.10,to provide a more reliable comparison of these amplification characteristics, the normalized Arias intensity was employed to define the effective duration of strong shaking. The characteristic times, t_5 and t_{95}, were identified as the points where the cumulative Arias intensity reached 5% and 95% of its final value, respectively. Consequently, the peak ground acceleration (*PGA*) values at each depth were recalculated exclusively within the t_5–t_{95} interval.

Using the PGA values calculated over this effective duration, the acceleration amplification factor was defined as $AF_{PGA}(z)=\frac{PGA(z)}{PGA(A1)}$, where $PGA(z)$ represents the peak acceleration at depth z, and $PGA(A1)$ denotes the peak acceleration recorded by the bottom reference sensor A1. To evaluate the relative amplification between the pile-reinforced and unreinforced ground, a ratio of the amplification factors was introduced: $R_A(z)=\frac{AF_{PGA,pile}(z)}{AF_{PGA,unreinforced}(z)}$. Accordingly, $R_A>1$ indicates that the pile-reinforced ground exhibits greater PGA amplification than the unreinforced ground at the same depth, whereas $R_A < 1$ signifies that the pile reinforcement mitigates the PGA amplification.

A pronounced decrease in R_A is also observed below the loose–dense sand interface, particularly at a depth of approximately 12.0 m. This phenomenon is likely attributable to the combined effects of pile

reinforcement and the stiffness contrast across the layer interface, which alter wave transmission and acceleration amplification characteristics. Consequently, the acceleration response provides primary evidence that the pile-reinforced ground did not behave as a uniformly restrained system under strong shaking. Rather, the localized reversal of the shallow response suggests that the kinematic compatibility between the rigid pile–cap system and the surrounding shallow soil diminished under the 0.26g input motion.

3.2 Shear Stress Response of Soil Layers

The soil shear response was analyzed to examine whether the acceleration-based shallow response reversal was accompanied by redistribution of shear demand and localized shear deformation. In this study, the one-dimensional equivalent shear beam method proposed by Zeghal et al. (1995) was adopted to calculate the horizontal shear stress time histories at different depths of the soil layers based on the measured acceleration responses in both the unreinforced ground and the pile-reinforced ground.The subsequent peak shear stress profiles and shear-stress ratio profiles were obtained from the calculated shear stresses at the corresponding depth positions.

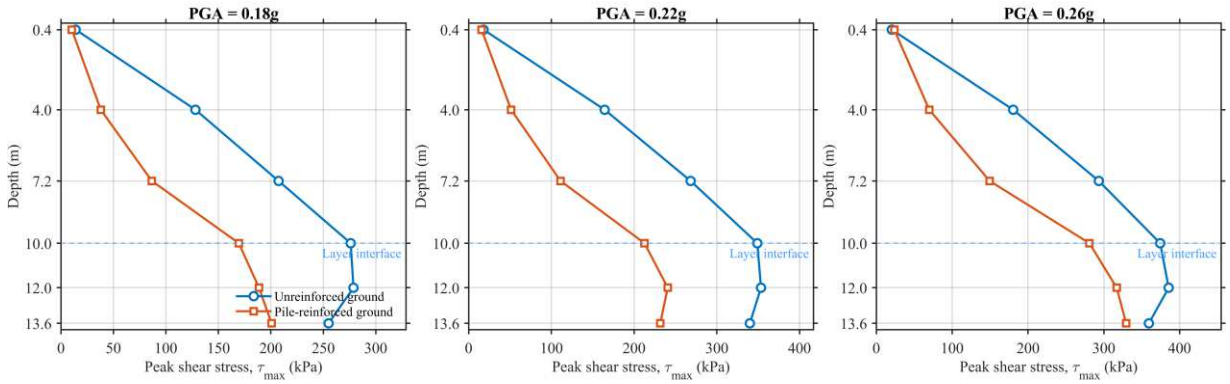


Fig.11.Peak shear stress profiles within the Arias intensity-based 5%–95% significant duration

Figure 11 shows that peak shear stress generally increases with depth in both ground conditions, reflecting higher seismic shear demands on deeper soil layers. The stress levels also escalate with input motion intensity, consistent with a stronger dynamic shear response under more intense shaking. Notably, a marked change in the stress profile occurs near the loose–dense sand interface for both models. Below this boundary, the gradient of stress increase becomes less steep, suggesting that the denser lower stratum modifies the transmission and accumulation of seismic shear stress.

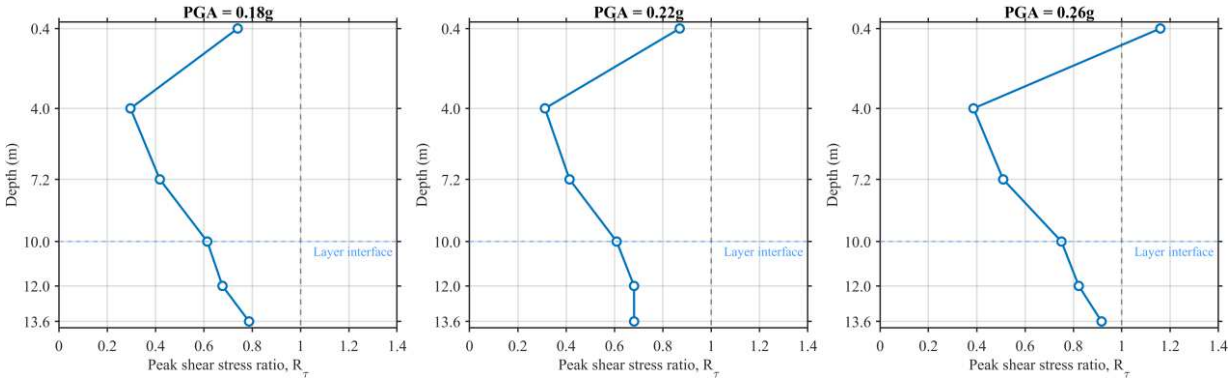


Fig.12. Peak shear stress ratio profiles within the Arias-intensity-based 5%–95% significant duration

To further quantify the influence of pile-group reinforcement on the shear response of the surrounding soil, the peak shear stress ratio,R_τ,was introduced. $R_\tau = \frac{\tau_{max,pile}}{\tau_{max,unreinforced})}$

This parameter is defined as the ratio of the peak shear stress in the pile-reinforced ground ($\tau_{max,pile}$) to that in the unreinforced ground ($\tau_{max,unreinforced}$).An $R_\tau$value less than unity signifies that the pile reinforcement reduces the peak shear stress at a given depth, whereas a value greater than unity indicates an amplification of shear stress relative to the unreinforced condition.

As depicted in Fig.12, the shear-stress ratio R_τ is predominantly below unity at most monitored depths under 0.18g and 0.22g input motions, indicating that pile-group reinforcement reduces the surrounding soil's shear stress under mild to moderate shaking intensities. Conversely, under the 0.26g motion,R_τ exhibits a more significant variation across the soil profile. While the reduction in shear stress remains prevalent in the mid-to-lower layers, the disparity between pile-reinforced and unreinforced grounds diminishes in shallow depths, where localized increments may occur. Collectively, these results imply that the observed reversal in shallow acceleration response is associated with redistributed soil shear demand rather than a uniform stress reduction throughout the depth.

3.3 Shear-strain response and shear stress–strain hysteresis loop

To examine shear deformation within the soil layers, shear strain was estimated from the relative displacement between adjacent accelerometer levels. The acceleration records were baseline-corrected and filtered before displacement was obtained by double integration. Although p–y hysteresis loops are commonly used to describe nonlinear pile–soil interaction (Rovithis et al. 2009; Boulanger et al. 1999), they could not be constructed because soil reaction and pile–soil relative displacement were not measured directly. Soil shear stress–strain loops were therefore used to identify deformation concentration, apparent stiffness changes, and the response associated with pile–soil deformation incompatibility.

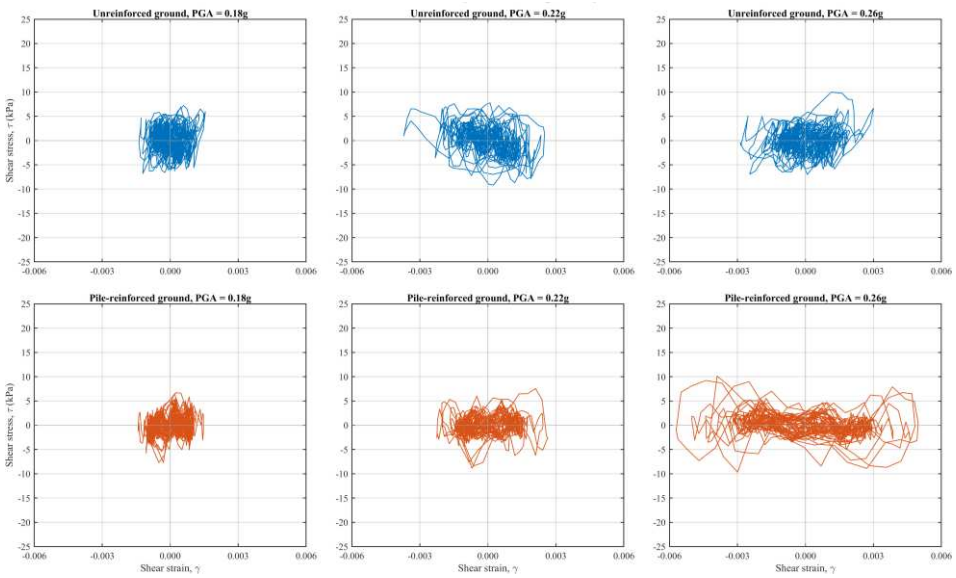


Fig.13. Shear stress–strain hysteresis loops at 2.2m under different input motions

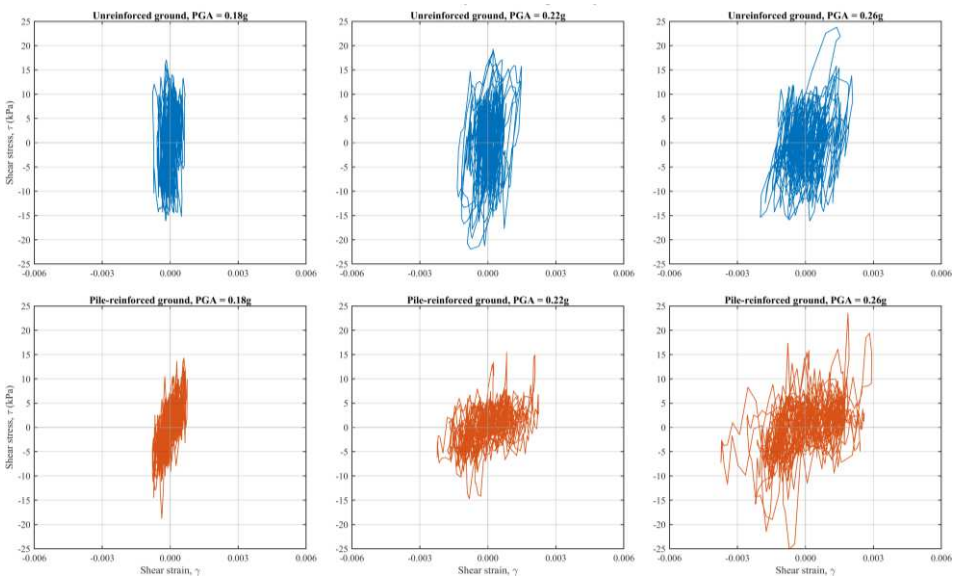


Fig.14. Shear stress–strain hysteresis loops at 7.2m under different input motions

The shear stress–strain hysteresis loops at depths of 2.2 m and 7.2 m are depicted in Figures 13 and 14, respectively. These depths were selected to represent the shallow and mid-upper soil layers, where pronounced pile‐soil deformation incompatibility was anticipated.

At 2.2 m depth, the hysteresis loops of unreinforced and pile-reinforced grounds exhibit minimal separation under 0.18g and 0.22g input motions, indicating negligible influence of pile reinforcement on shear deformation concentration under mild-to-moderate shaking. However, under the 0.26g motion, the loop for the reinforced ground expands more prominently in the shear strain direction, despite limited proportional growth in shear stress amplitude. This behavior signifies intensified cyclic shear deformation and reduced apparent stiffness in the shallow reinforced layer subjected to strong shaking.

At 7.2 m depth, the hysteresis loops similarly enlarge with increasing input motion intensity, reflecting intensified soil shear response under severe shaking. However, compared to the 2.2 m depth,

the distinction between unreinforced and reinforced grounds is less conspicuous at 7.2 m. This suggests that the enhanced shear deformation in the reinforced ground is primarily confined to shallow depths, gradually attenuating with increasing depth.

Overall, these findings contradict full-depth weakening of the reinforced ground under strong shaking. Instead, the 0.26g motion triggers depth-dependent shear deformation localization in shallow-to-mid-upper soil layers. This deformation pattern aligns with observed acceleration reversals in shallow regions, supporting the hypothesis that such reversals stem from localized pile–soil deformation incompatibilities.

3.4 Discussion: mechanism of localized pile–soil deformation incompatibility

The combined results show that the reinforced-ground response reflected competition between pile-group restraint and localized pile–soil kinematic incompatibility. Under the 0.18g and 0.22g motions, the pile group generally reduced PGA amplification, while the two grounds exhibited similar shear-strain ranges, indicating relatively compatible deformation and a dominant restraining effect. Under the 0.26g motion, however, acceleration response reversal occurred in the shallow reinforced soil, whereas the deeper layers remained restrained. The enlarged shallow hysteresis loops, without a proportional increase in shear stress, further indicate localized cyclic deformation and apparent stiffness degradation rather than full-depth weakening.

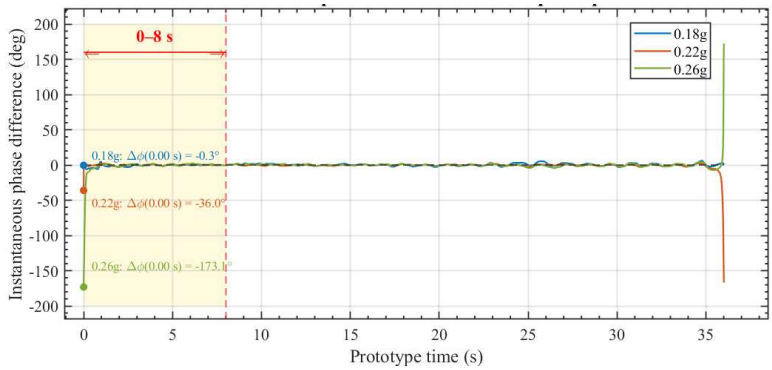


Fig.15.Instantaneous acceleration phase difference between the pile cap and shallow soil under different input motions.

The instantaneous displacement phase difference provides direct evidence of this motion incompatibility. As shown in Fig.15, distinct negative phase differences occur at the onset of all three shaking events, indicating that the shallow soil initially lagged behind the pile-cap motion under the adopted sign convention. The initial phase-difference magnitude increased with input intensity and reached $-173.1°$ under the 0.26g motion. Thereafter, the phase difference decreased rapidly and fluctuated around zero, indicating that the pronounced motion incompatibility was transient and that the pile cap and shallow soil gradually entered a more coordinated response stage.

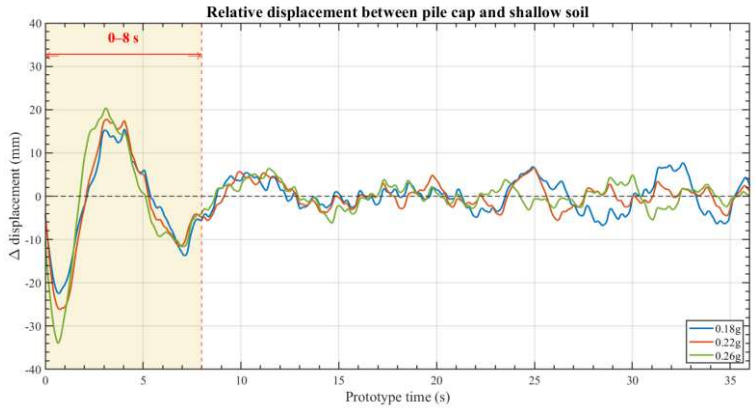


Fig.16. Relative displacement between the pile cap and shallow soil under different input motions.

The relative displacement histories in Fig.16 show a consistent response pattern. Large pile-cap–soil relative displacement developed during the early stage of shaking and remained pronounced before the first major response peak, approximately within the initial 0–8 s interval. Its amplitude increased with input intensity, confirming that stronger shaking intensified the initial kinematic incompatibility between the pile cap and the shallow soil.

This behavior can be attributed to pile-cap inertia, shallow-soil softening, and the resulting stiffness contrast. The relatively rigid pile–cap system responded rapidly, whereas cyclic shearing reduced the apparent stiffness of the shallow sand and delayed its motion. The resulting relative movement caused repeated lateral squeezing and shearing of the inter-pile soil, increasing local deformation demand and contributing to the shallow acceleration response reversal under the 0.26g motion. At greater depths, higher confinement and stronger pile embedment restraint limited soil deformation, so the stiffness effect of the pile group remained dominant.

Therefore, the shallow response reversal should be interpreted as a localized consequence of transient pile–soil kinematic incompatibility rather than a loss of reinforcement effectiveness throughout the soil profile. Seismic evaluation of capped non-displacement pile groups should consider both their overall restraining effect and the possibility of localized shallow amplification under strong shaking.

4 Conclusion

Based on the centrifuge shaking-table tests on unreinforced dry sand and dry sand reinforced with a capped 3 × 6 non-displacement pile group, the following conclusions are drawn:

(1) Under the 0.18g and 0.22g motions, the pile group generally reduced PGA amplification during the 5%–95% Arias-intensity duration. Under the 0.26g motion, however, the shallow reinforced soil exhibited greater acceleration amplification than the unreinforced soil, while the deeper layers remained restrained. The pile-group effect therefore varied markedly with depth under strong shaking.

(2) The shallow response reversal was associated with localized deformation concentration rather

than full-depth weakening. Shear-stress reduction persisted in the middle and lower layers under the 0.26g motion, whereas the difference between the two models diminished near the surface. The shallow inter-pile soil also developed a wider shear-strain range without a proportional increase in shear stress, indicating intensified cyclic deformation and reduced apparent stiffness.

(3) The governing response reflected competition between the restraining effect of pile-group stiffness and localized pile–soil kinematic incompatibility. At lower shaking intensities, the pile–cap system and surrounding soil deformed relatively compatibly, allowing the piles to restrain soil motion. Under strong shaking, pile-cap inertia, shallow-soil softening, stiffness mismatch, and repeated lateral pile–soil interaction promoted localized deformation in the upper soil layers. Seismic design of large capped non-displacement pile groups should therefore consider both their overall reinforcing effect and the potential for shallow response amplification.

Acknowledgements The authors gratefully acknowledge the technical support provided by the centrifuge laboratory of the China Institute of Water Resources and Hydropower Research.

Author Contributions Pengkun Rao: Investigation, Data curation, Formal analysis, Visualization, Writing – original draft. Xuedong Zhang, Rui Wang,Yanpeng Sun and Weizhe Meng: Supervision, Resources, Writing – review and editing. All authors read and approved the final manuscript.

Funding The authors received no funding for this work.

Data Availability The datasets generated and analyzed in this study may be provided by the corresponding author upon reasonable request.

Declarations

Competing Interest The authors have no relevant financial or non-financial interests to disclose.

References

Aghamolaei M, Saeedi Azizkandi A, Abolhasanpoor A, Hashemi S (2024a) Influence of soil–pile interfa ce characteristics on the seismic response of single pile foundations: shaking table testing and numerical sim ulation. Acta Geotech 19(1):417–436. https://doi.org/10.1007/s11440-023-01955-9

Aghamolaei M, Saeedi Azizkandi A, Abolhasanpoor A (2024b) Kinematic internal forces of free-head si ngle piles subjected to seismic loading: shaking table testing and numerical simulation. Int J Civ Eng 22(5):8 01–821. https://doi.org/10.1007/s40999-023-00915-4

Ahmadi MM, Hadei S, Borzeshi SA, Hokmabadi A (2025) Effects of loading frequency on soil–pile inte raction using numerical nonlinear three-dimensional analyses. Int J Geomech 25:04024301. https://doi.org/10.1 061/IJGNAI.GMENG-10119

Boulanger RW, Curras CJ, Kutter BL, Wilson DW, Abghari A (1999) Seismic soil-pile-structure interacti on experiments and analyses. J Geotech Geoenviron Eng 125(9):750–759. https://doi.org/10.1061/(ASCE)1090

-0241(1999)125:9(750)

Chau KT, Shen CY, Guo X (2009) Nonlinear seismic soil–pile–structure interactions: Shaking table tests and FEM analyses. Soil Dyn Earthq Eng 29:300–310. https://doi.org/10.1016/j.soildyn.2008.02.004

Fan K, Gazetas G, Kaynia A, Kausel E, Ahmad S (1991) Kinematic seismic response of single piles and pile groups. J Geotech Eng 117:1860–1879. https://doi.org/10.1061/(ASCE)0733-9410(1991)117:12(1860)

He Z, Jiang G, Huang H (2026) A damage-cumulative dynamic interaction model for pile–soil–anchor cable systems: Development and verification via shaking table tests. Soil Dyn Earthq Eng 207:110354. https://doi.org/10.1016/j.soildyn.2026.110354

Hussien MN, Tobita T, Iai S, Karray M (2016) Soil–pile–structure kinematic and inertial interaction observed in geotechnical centrifuge experiments. Soil Dyn Earthq Eng 89:75–84. https://doi.org/10.1016/j.soildyn.2016.08.002

Lee YG, Adeel MB, Park D (2026) Numerical simulations of seismic response of pile foundations in sand using 3D finite element methods. Geomech Eng 44:513–527. https://doi.org/10.12989/gae.2026.44.4.513

Nikolaou S, Mylonakis G, Gazetas G, Tazoh T (2001) Kinematic pile bending during earthquakes: Analysis and field measurements. Géotechnique 51:425–440. https://doi.org/10.1680/geot.2001.51.5.425

Nohra C, Li Z, Escoffier S, Thorel L (2026) Numerical investigation of the effects of kinematic interaction in rigid inclusion reinforced soft ground. Soil Dyn Earthq Eng 206:110248. https://doi.org/10.1016/j.soildyn.2026.110248

Padmanabhan G, Ueda K, Maheshwari BK, Uzuoka R (2024) Reliquefaction behavior of sand and response of pile group subjected to repeated shaking sequence using centrifuge model experiments. Soil Dyn Earthq Eng 182:108741. https://doi.org/10.1016/j.soildyn.2024.108741

Rodríguez-Galván E, Carbonari S, Dezi F, Álamo GM, Aznárez JJ, Maeso O, et al (2026) Lateral kinematic response of single-pile bridge pier foundations under seismic waves: Linear versus non-linear soil behavior. Soil Dyn Earthq Eng 208:110411. https://doi.org/10.1016/j.soildyn.2026.110411

Rovithis E, Kirtas E, Pitilakis K (2009) Experimental p-y loops for estimating seismic soil-pile interaction. Bull Earthq Eng 7:719–736. https://doi.org/10.1007/s10518-009-9116-7

Sawamura Y, Inagami K, Nishihara T, Kosaka T, Hattori M, Kimura M (2021) Seismic performance of group pile foundation with ground improvement during liquefaction. Soils Found 61:944–959. https://doi.org/10.1016/j.sandf.2021.06.010

Stacul S, Rovithis E, Di Laora R (2022) Kinematic soil–pile interaction under earthquake-induced nonlinear soil and pile behavior: An equivalent-linear approach. J Geotech Geoenviron Eng 148:04022055. https://doi.org/10.1061/(ASCE)GT.1943-5606.0002813

Tamura S, Ohno Y, Shibata K, Funahara H, Nagao T, Kawamata Y (2021) E-Defense shaking test and pushover analyses for lateral pile behavior in a group considering soil deformation in vicinity of piles. Soil Dyn Earthq Eng 142:106529. https://doi.org/10.1016/j.soildyn.2020.106529

Tokimatsu K, Suzuki H, Sato M (2005) Effects of inertial and kinematic interaction on seismic behavior of pile with embedded foundation. Soil Dyn Earthq Eng 25:753–762. https://doi.org/10.1016/j.soildyn.2004.11.018

Tran NX, Bong T, Kim SR (2022) Kinematic and inertial interaction of single and group piles in slope by displacement phase relation. J Earthq Eng 26:3639–3659. https://doi.org/10.1080/13632469.2020.1813661

Yang Z, Zhang S, Liu H, Liu M, Li Y, Guan Q (2026) Seismic response and failure mechanism of pile foundations at different relative positions and rock-socketed depths on deep deposit slopes. Eng Geol 364:108604. https://doi.org/10.1016/j.enggeo.2026.108604

Yun JW, Han JT (2023) Evaluation of the dynamic behavior of pile groups considering the kinematic force of

the slope using centrifuge model tests. Soil Dyn Earthq Eng 173:108106. https://doi.org/10.1016/j.soildyn.2023.108106

Zeghal M, Elgamal AW, Tang HT, Stepp JC (1995) Lotung Downhole Array. II: Evaluation of soil nonlinear properties. J Geotech Eng 121(4):363–378. https://doi.org/10.1061/(ASCE)0733-9410(1995)121:4(363)

Zhan H, He W, Yang J, Ding Z, Wang K, Yu H (2026) Improved Penzien theoretical model for pile groups and dynamic response analysis of nuclear power plants on non-bedrock foundations. Soil Dyn Earthq Eng 204:110150. https://doi.org/10.1016/j.soildyn.2026.110150

Zhang X, Lv X, Qin Z, Zuo S, Wang W, Luo Q, et al (2025) Shake-table test study of dynamic response of soil–pile interaction system in seasonally frozen soil regions. J Geotech Geoenviron Eng 151:04025010. https://doi.org/10.1061/JGGEFK.GTENG-12890

Zheng G, Zhang W, Forcellini D, Zhou H, Zhao J (2024) Dynamic centrifuge modeling on the superstructure–pile system considering pile–pile cap connections in dry sandy soils. Soil Dyn Earthq Eng 187:108979. https://doi.org/10.1016/j.soildyn.2024.108979